Thermoelectric and optical properties of the filled skutterudite YbFe$_4$Sb$_{12}$

N. R. Dilley, E. D. Bauer, and M. B. Maple

Department of Physics and Institute for Pure and Applied Physical Sciences, University of California, San Diego,
La Jolla, California 92093

S. Dordevic and D. N. Basov

Department of Physics, University of California, San Diego, La Jolla, California 92093

F. Freibert, T. W. Darling, and A. Migliori

Los Alamos National Laboratory, Los Alamos, New Mexico 87545

B. C. Chakoumakos and B. C. Sales

Solid State Division, Oak Ridge National Laboratory, Oak Ridge, Tennesse 37831
(Received 18 June 1999; revised manuscript received 28 September 1999)

Transport measurements, including magnetoresistivity, Hall resistivity, thermal conductivity, and thermopower, and an assessment of the dimensionless thermoelectric figure of merit ZT below room temperature are reported on a polycrystalline sample of the strongly correlated electron material YbFe$_4$Sb$_{12}$. Neutron diffraction measurements are presented, which reveal large amplitude thermal vibrations of the Yb ion, consistent with speculations that the ion is weakly bound in an oversized atomic ''cage'' formed in the skutterudite crystal structure. Infrared spectroscopy measurements reveal a resonance in the dissipative part of the optical conductivity $\sigma_1(\omega)$, which develops below $T^* \approx 70$ K, the characteristic temperature for the Yb ion valence fluctuations. The frequency dependence of the optical constants is suggestive of a hybridization band gap in the quasiparticle density of states at low temperatures.

I. INTRODUCTION

Since they were first synthesized in the 1970s,[1] the filled skutterudite compounds RT_4X_{12} (where R=Ca, Sr, Ba, La-Eu, Yb, Th, U; T=Fe, Ru, Os; X=pnictogen: P, As, Sb) have been of interest to experimentalists and theorists alike. These compounds derive many of their remarkable properties from the heavy-R ion that occupies an atomic ''cage'' in the traditional (''unfilled'') CoAs$_3$-type skutterudite structure: magnetism,[2] superconductivity,[3] narrow hybridization bandgap semiconductivity,[4] heavy-fermion behavior,[5,6] and a metal-insulator transition[7] are some of the phenomena that can arise. The latter three examples of strongly correlated electronic effects occur in compounds containing R atoms such as Ce, Yb, and U which have unstable f-electron shells.

Skutterudites have also been identified recently as promising candidates for thermoelectric applications,[8] i.e., solid-state refrigeration by passing an electrical current (Peltier effect) or power generation by using waste heat (Seebeck effect). The ''figure of merit'' of a thermoelectric material is expressed as $Z = S^2/(\rho\kappa)$, where S is the Seebeck coefficient, ρ is the electrical resistivity, and κ is the thermal conductivity, and viability is achieved roughly when the so-called ''dimensionless figure of merit'' $ZT \gtrsim 1$ where T is the operating temperature. The observation of high-carrier mobilities μ and thermoelectric ''power factors'' (S^2/ρ) in unfilled skutterudites such as hole-doped (p-type) CoSb$_3$,[9] along with the subsequent demonstration of extremely low-thermal conductivities in filled skutterudites, led Sales and coworkers[10] to an encouraging $ZT \approx 1$ near T=800 K in chemically doped filled skutterudites. In general, optimal thermoelectric properties are achieved in doped semiconductors when enough charge carriers keep the resistivity at a moderate level, but not too many as to lower the Seebeck coefficient to the values typically found in metals. The ability to chemically dope the filled skutterudites, which are generally metallic or semi-metallic, into this semiconducting regime is essential to their thermoelectric applicability, and this has been demonstrated by several recent studies.[11–13] Suppressing the lattice contribution to the thermal conductivity while maintaining good electrical conduction, i.e., strongly scattering phonons but not charge carriers, is another challenge, and the filled skutterudites appear to derive their favorable qualities due to the presence of the filling atoms (R), which ''rattle'' with large amplitudes in their atomic cages.[14,15] It has been suggested[10,16] that localized, incoherent vibrations of the loosely bound filler atoms scatter phonons effectively, but remain spatially separated from the electronic transport that is thought to occur within the metal-pnictogen sublattice.

To highlight yet another attribute of these materials that is appealing for thermoelectric devices, we return to the observation of strong electronic correlations and, specifically, of heavy fermion (HF) and hybridization gap phenomena in certain filled skutterudites. A salient feature of many HF metals is the existence of an anomalously large Seebeck coefficient that peaks in the vicinity of the coherence temperature T^* of the compound, i.e., the temperature below which charge carrier scattering is suppressed due to coherence in the ''Kondo lattice'' of f-electron ions that carry magnetic moments. In hybridization gap materials, also termed Kondo insulators, the hybridization of a narrow f level with a broad $s-p$ metallic band can produce a narrow gap in the elec-

tronic density of states at the Fermi level. According to theoretical calculations,[17] this situation of a large density of states close to the gap can set the stage for optimal thermoelectric properties.

Reported in this paper are the transport, structural, and optical properties of the recently discovered filled skutterudite compound $YbFe_4Sb_{12}$.[18] Our initial reports[18,19] indicated that this compound shared many properties with the heavy fermion $CeFe_4Sb_{12}$, exhibiting a crossover temperature $T^* \approx 70$ K, interpreted in terms of intermediate valence behavior of the Yb ion with a nonmagnetic ground state. A similar energy scale was found in $CeFe_4Sb_{12}$ and was described in terms of Kondo coherence on the Ce sublattice,[6,19] which is a way of expressing nearly identical results but is appropriate to the case where the magnetic moment (Ce^{3+}) is stable. The present work investigates the optical signature of this many-body interaction at T^*, and also reports on the thermoelectric properties of $YbFe_4Sb_{12}$ and their correlation to the ''rattling'' of the Yb ion as measured by neutron diffraction.

II. EXPERIMENTAL DETAILS

Polycrystalline specimens of $YbFe_4Sb_{12}$ were synthesized by induction melting stoichiometric amounts of elemental constituents in a graphite crucible in a UHP Ar atmosphere, and annealing for about 35 hours at 600°C (for more details, see Ref. 18). Investigation of several samples by a scanning electron microscope revealed significant porosity (samples were found to be approximately 80% of theoretical density) and typical grain sizes of 10 μm. Energy dispersive x-ray (EDX) analysis indicated that the composition within the grains was correct to within the error of the technique, and EDX was also used to identify a trace (less than 5 vol.%) secondary phase as $YbSb_2$, which was reported earlier[18] in powder x-ray diffraction data.

For electrical transport measurements made at Los Alamos National Laboratory, the samples were cut in a rectangular parallelepiped shape having width (W), height (H), and length (L) dimensions of $2.0 \times 2.0 \times 8.0$ mm^3, respectively. This specimen geometry minimizes electrical shorting of the Hall effect.[20] Longitudinal and Hall resistivity was measured with 40 gauge Cu wire leads, which were attached using EPO-TEK H20E silver epoxy, and the sample was held between two copper plates with the addition of silver paint for improved electrical contact. Using a swept source technique, the longitudinal and transverse voltages were plotted as functions of the electrical current and the slope of linear fits to these data provided the longitudinal and transverse resistivities. This procedure was carried out at both $B = 0$ and $B = 3$ tesla.

Thermal transport data from 10–300 K were obtained at the Oak Ridge National Laboratory (ORNL) using a closed cycle helium refrigerator. The sample was suspended from a copper cold finger using EPO-TEK H20E silver epoxy. A small RuO_2 chip resistor (51 Ω) was attached to the other end of the sample using a thermally conducting but electrically insulating epoxy from EPO-TEK (930-4). Electrical connections were soldered to the heater (0.075 mm chromel wires). Small temperature differences (1–3 K) across the sample were measured using two 0.125 mm chromel-constantan thermocouples attached to the sample using Dupont 4929N silver paste. For Seebeck measurements, two 0.075-mm copper wires were attached to the sample with silver paste. The sample and wires were enclosed in a copper can that was thermally attached to the cold finger. The copper can was at approximately the same temperature as the cold end of the sample. Using this arrangement, radiation losses were kept to a minimum. Typically, a constant current of 10 mA was passed through the heater, and, at each temperature, the thermal gradient was allowed to stabilize for 30 min. The thermal conductivity and Seebeck coefficient was then measured. For samples with values for thermal conductivity of 100 mW/cm-K and above, the radiation and conduction losses were small enough to be neglected regardless of the geometry of the sample. However, many of the filled skutterudites have thermal conductivities (at room temperature) in the 15–30 mW/cm-K range. To obtain reliable thermal conductivity values for these materials, all of the copper leads were removed from the sample and the samples were cut into a specific shape ($6 \times 6 \times 12$ mm^3), which had a relatively large ratio of the cross-sectional area to length. It was found that this procedure yielded the correct thermal conductivity values for a vitreous SiO_2 standard over the entire 10–300 K temperature interval.

Neutron scattering measurements were carried out at the ORNL High Flux Isotope Reactor in a neutron diffractometer equipped with a closed-cycle liquid helium refrigerator. Powder diffractograms using a wavelength of 1.500 Å were collected at $T = 10, 40, 60, 80, 140, 200,$ and 300 K, and refined using the Rietveld method and the program GSAS (General Structure Analysis System) developed by Larson and von Dreele at Los Alamos National Laboratory.[21]

The electrodynamic response of polished samples of $YbFe_4Sb_{12}$ was studied at UCSD using infrared and optical reflectance spectroscopy. Near normal incidence reflectance $R(\omega)$ of polycrystalline samples was measured in the frequency range 50–30 000 cm^{-1} (approximately 5 meV–3 eV) from $T = 10$ K to room temperature. Samples were coated *in situ* in the optical cryostat with gold or aluminum and the spectrum of a metal-coated sample was used as a reference. The complex conductivity $\sigma(\omega) = \sigma_1(\omega) + i\sigma_2(\omega)$ was obtained from $R(\omega)$ using Kramers-Kronig analysis, and the uncertainty in $\sigma(\omega)$ due to both low- and high-frequency extrapolations required for Kramers-Kronig analysis was negligible in the frequency range of the data.

III. RESULTS AND DISCUSSION

The transport properties of $YbFe_4Sb_{12}$ were measured from room temperature down to $T = 10$ K and are shown in Fig. 1. The longitudinal electrical resistivity is shown as filled symbols in Fig. 1(c) and agrees qualitatively with our previous data, although this sample shows a smaller residual resistivity ratio $RRR = \rho(300 \text{ K})/\rho(0 \text{ K}) \approx 7$ compared with $RRR \approx 12$ in the previous sample.

Note that no corrections for sample porosity were made for in these measurements, which leads to an overestimation of the resistivity. Transverse magnetoresistance, defined as $\Delta\rho/\rho_0 = [\rho(B) - \rho(0)]/\rho(0)$ where $B = 3$ tesla is the applied magnetic field, is shown by the filled symbols in Fig. 1(a). A large positive magnetoresistance develops below $T \approx 50$ K,
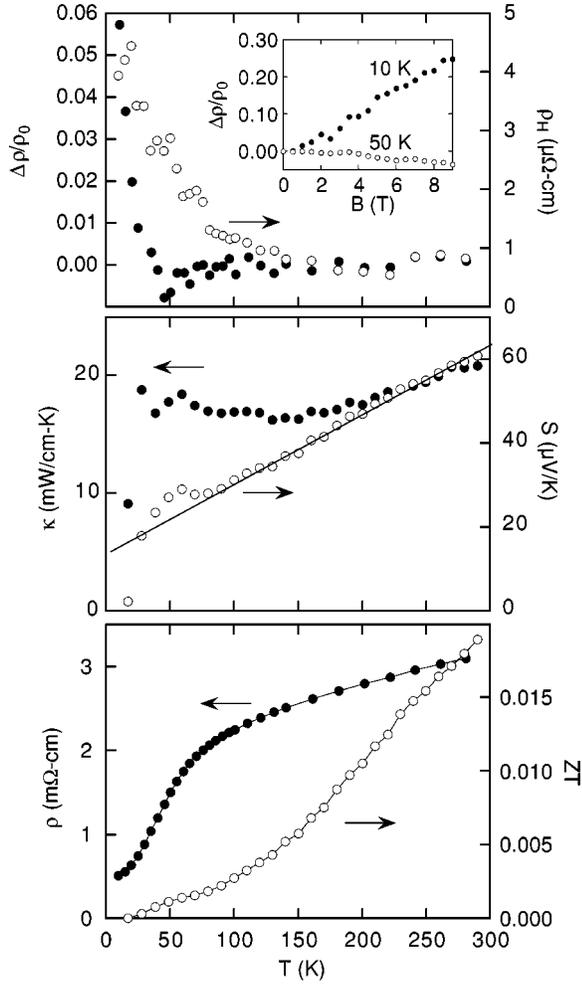
FIG. 1. Transport properties of YbFe$_4$Sb$_{12}$ as a function of temperature T. Upper panel: transverse magnetoresistivity $\Delta\rho/\rho_0$ (filled symbols, left-hand axis) and Hall resistivity ρ_H (open symbols, right-hand axis), both measured in an applied magnetic field of $B = 3$ tesla. Inset shows field sweeps of the magnetoresistivity $\Delta\rho/\rho_0$ at $T = 10$ and 50 K. Middle panel: thermal conductivity κ (filled symbols, left-hand axis) and Seebeck coefficient S (open symbols, right-hand axis). Lower panel: electrical resistivity (filled symbols, left-hand axis) and dimensionless thermoelectric figure of merit $ZT = S^2T/(\rho\kappa)$ (open symbols, right-hand axis).

but is preceded by a slight negative excursion in the vicinity of $T^* \approx 70$ K, which is the characteristic temperature of the Yb ion valence fluctuations as inferred from previous measurements of magnetization and electrical resistivity. The small negative feature seen in $\Delta\rho/\rho_0$ was clearly corroborated by other magnetoresistance measurements on this sample using a different experimental setup. The general appearance of the magnetoresistance is reminiscent of the heavy fermion compound CeCu$_6$, although the characteristic temperature here is higher. The negative feature seen near T^* is consistent with single-ion Kondo scattering in that the applied magnetic field acts to suppress the spin-flip scattering of conduction electrons by the magnetic ion. On the other hand, the formation of a coherent ground state in the Kondo lattice removes the Kondo scattering and leads to a positive magnetoresistance which is typical of metals. Note that the value of $\Delta\rho/\rho_0 > 0.05$ in this region is much larger than in simple metals where $\Delta\rho/\rho_0 \sim 10^{-6}$, but is similar to other

Kondo lattice materials. The inset of Fig. 1(a) shows the magnetic field dependencies of $\Delta\rho/\rho$ in the single-ion (50 K) and coherent (10 K) regimes which were monotonic and roughly linear in high fields ($B > 4$ tesla).

Shown by the open symbols in Fig. 1(a) is the Hall resistivity ρ_H measured at $B = 3$ tesla, which is positive and increases monotonically with decreasing temperature. The qualitative features of the data seem to be at variance with many heavy-fermion systems such as CeCu$_6$ and UPt$_3$ in which the Hall resistivity decreases strongly in the coherent regime, although an abrupt downturn might occur below $T = 25$ K and warrants further study. The data are similar to those obtained for CeFe$_4$Sb$_{12}$ (see Ref. 12), which has also been interpreted as a moderately heavy-fermion material.[5,6,19] The observation of a positive Hall coefficient, i.e., electrical conduction by holes, in both of these compounds is consistent with a simple electron-counting scheme based on the parent compound CoSb$_3$ being a semiconductor. As iron possesses one fewer electron than cobalt, the polyanion $[\text{FeSb}_3]^{4+}$ is formed, thus requiring a tetravalent filling ion R to produce a compensated semiconducting material $R\text{Fe}_4\text{Sb}_{12}$. However, measurements of both the cubic lattice parameter and bulk magnetization indicate that Ce is nearly trivalent, and Yb has an intermediate valence significantly less than trivalent in these compounds, implying hole conduction. An estimate of the effective hole concentration p_{eff} can be obtained by assuming single-band conduction: $p_{\text{eff}} = B/\rho_H e = 3 \times 10^{21}$ cm^{-3} at $T = 100$ K, which corresponds to about 1.2 holes per formula unit. This value is roughly consistent with the carrier concentration estimated from optical data. The Hall mobility estimated at room temperature is $\mu = \rho_H/B\rho_{xx} \approx 0.7$ cm^2/(V-s).

Although the electron-counting scheme seems to correctly predict the sign of charge carriers, it fails to explain the metallic behavior of ThFe$_4$P$_{12}$ in which thorium is known to be tetravalent. In addition, lattice parameter measurements provide evidence for cerium ion intermediate valence in the compounds CeT_4P$_{12}$ ($T = $Fe and Ru), which are the only semiconducting members of the lanthanide filled skutterudites. For these reasons, it was previously proposed that the semiconductivity in filled skutterudites $R\text{Fe}_4\text{P}_{12}$ ($R = $Ce and U) arises from f-electron hybridization effects and not simple ionic bonding arguments.[4,22] The thermal conductivity κ of YbFe$_4$Sb$_{12}$, shown by the solid symbols in Fig. 1(b), is comparable to other filled skutterudites [for CeFe$_4$Sb$_{12}$ at 300 K, $\kappa \approx 30$ mW/(cm-K)].[12] Correcting for sample porosity would increase the estimate of κ by 15–20 %. Expressing κ as the sum of lattice and electronic thermal conductivities, $\kappa = \kappa_L + \kappa_e$, and estimating κ_e with the help of the Wiedemann-Franz law, we find that κ_L dominates thermal conduction due to the high value of the measured electrical resistivity, with $\kappa_e(300 \text{ K}) = 2.3$ mW/(cm-K). The sharp downturn in both κ and S at the lowest temperature is due to the depopulation of phonon modes and is expected since $\kappa(T=0) = S(T=0) = 0$.

The Seebeck coefficient S is plotted as open symbols in Fig. 1(b) and shows linear behavior at high temperature typical of a low-carrier density metal, behavior that is seen in other filled skutterudite compounds. The slope of the linear, high-temperature thermopower S_d, which is characteristic of

electron thermal diffusion, can be used to find the Fermi energy E_F

$$S_d = \frac{\pi^2 k_B^2 T}{e E_F}, \qquad (1)$$

where we have used the expression appropriate to the regime where the resistivity is dominated by phonon scattering. This yields a value of $E_F = 0.42$ eV, which is lower than in wideband metals and more typical of semimetals. Extrapolating this fit to zero temperature, one finds a positive y intercept, which indicates that the high temperature slope of S_d is underestimated here, i.e., E_F is overestimated. Viewed along with the observations of intermediate valence and hole conduction in this compound, one is led to a model of a nearly full band with f-electron character. The hump in $S(T)$ seen around 50 K could be a so-called "phonon drag" peak resulting from the interaction of carriers with thermally diffusing phonons. Such a peak in $S(T)$ is expected to occur near $\Theta_D/5 \approx 55$ K,[23] where the Debye temperature $\Theta_D \approx 280$ K has been estimated from high temperature specific heat measurements.[24] However, the fact that such a low-temperature feature has only been observed in Ce- and Yb-filled skutterudites, which exhibit strongly correlated electron phenomena suggests, that it is of the same origin as the Kondo coherence peaks in $S(T)$ seen in other HF compounds.

The dimensionless thermoelectric figure of merit $ZT = S^2 T/\rho\kappa$ is small in this compound [open symbols in Fig. 1(c)] when compared to other undoped filled skutterudites such as $CeFe_4Sb_{12}$ ($ZT \approx 0.13$ at $T = 300$ K according to Ref. 5), and this can be attributed to the relatively high value of the resistivity. Measurements of the infrared reflectivity reported here, however, extrapolate to a value of the intrinsic dc electrical resistivity at $T = 300$ K which is an order of magnitude lower (see Fig. 4) than the bulk transport data of Fig. 1(c), indicating that higher values of ZT may be attainable in clean samples. The electronic coherence effects seen in $S(T)$ near T^* do little to enhance ZT, giving rise to a broad shoulder near $T = 50$ K.

Neutron diffraction measurements show evidence of large-amplitude thermal "rattling" of the Yb ion in $YbFe_4Sb_{12}$, a mechanism thought to be responsible for the generally low-thermal conductivities found among filled skutterudites. Detailed crystallographic analysis of x-ray or neutron diffraction data can provide information about local dynamics such as the atomic displacement parameters (ADP's), which quantify the vibrational mean squared displacement of each atom in the structure from its equilibrium position and are expressed in units of Å^2. Shown in Fig. 2 are the results of a Rietveld analysis of neutron powder diffractograms, which tracked U_{iso}, the isotropic ADP averaged over all spatial directions, for each element in the material as a function of temperature. Within this analysis, the atomic vibrations of Yb appear to be much larger than those of both Fe and Sb, and in fact the U_{iso} for Yb at room temperature is the highest for any of the skutterudites RFe_4Sb_{12} ($R=$ Yb, Ce, La) measured by this technique. It is of interest to compare the dynamics of Yb to the significantly lighter lanthanides La and Ce in finding an optimal filling atom with respect to the "rattling" effect. Static disorder at the Yb site,
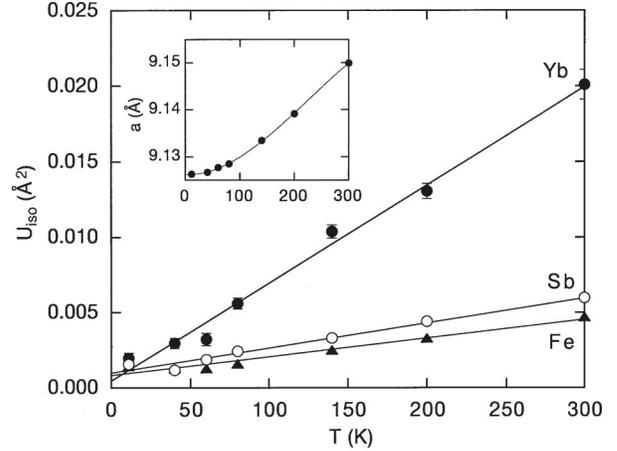

FIG. 2. Isotropic atomic displacement parameters U_{iso} obtained from Rietveld refinement of neutron diffraction data, plotted as a function of temperature for each element in $YbFe_4Sb_{12}$. The straight lines are least squares fits of the data for each site. The inset shows the temperature dependence of the cubic lattice parameter and the curve is a guide to the eye.

e.g., incomplete filling, will also result in a large U_{iso} but one that will remain large even as $T \rightarrow 0$, and the fact that U_{iso} linearly approaches zero at low temperatures is evidence against such disorder. The Yb filling fraction was also checked in a separate analysis by allowing the Yb site occupation parameter to vary in the Rietveld analysis of each diffractogram, yielding 95% filling. We note that a recent report on x-ray structural analysis of single-crystalline $YbFe_4Sb_{12}$ cites a large ADP at the Yb site in agreement with our findings.[25] Neutron diffraction also found no evidence of structural or magnetic transitions between room temperature and 10 K, and the inset of Fig. 2 shows the cubic lattice parameter a as a function of temperature. Impurity phases identified in the neutron data include $FeSb_2$ (4 wt. %) and $YbSb_2$ (0.5 wt. %).

Plotted in Fig. 3 is the raw reflectance data $R(\omega)$ at two temperatures, both above and below $T^* \approx 70$ K. As can be seen from the graph, there is no temperature dependence in the reflectance above 1000 cm^{-1}. The low-frequency extrapolation was performed using the Hagen-Rubens equation

$$R(\omega) = 1 - \sqrt{\frac{2\omega\rho_{dc}}{\pi}}. \qquad (2)$$

The inset shows room temperature data down to 40 cm^{-1} and a fitted Hagen-Rubens extrapolation by the solid line. We point out that the only fitting parameter $\rho_{dc} = 400$ $\mu\Omega$-cm could be determined within an error of less than 10% as shown by the dashed lines on either side of the extrapolation that was used.

Since the absolute values of the dc electrical resistivity ρ_{dc} for this sample (not shown) were not known from transport measurements, we used the absolute value obtained from Hagen-Rubens extrapolation at room temperature to normalize the transport data. We then used the normalized values of $\rho_{dc}(T)$ to perform the Hagen-Rubens extrapolations for the other temperatures.
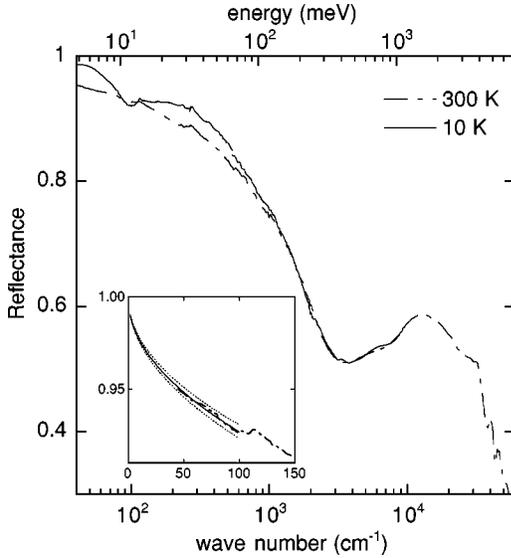
FIG. 3. Raw reflectance data at room temperature and $T = 10$ K. The data at frequencies above 2500 cm^{-1} did not show any temperature dependence. The inset illustrates the low frequency Hagen-Rubens extrapolation as applied to the room temperature data, where the solid line is the best fit for which the only fitting parameter was $\rho_{dc} = 400$ $\mu\Omega$-cm. The dashed lines are the extrapolations using $\rho_{dc} = 440$ and 360 $\mu\Omega$-cm.
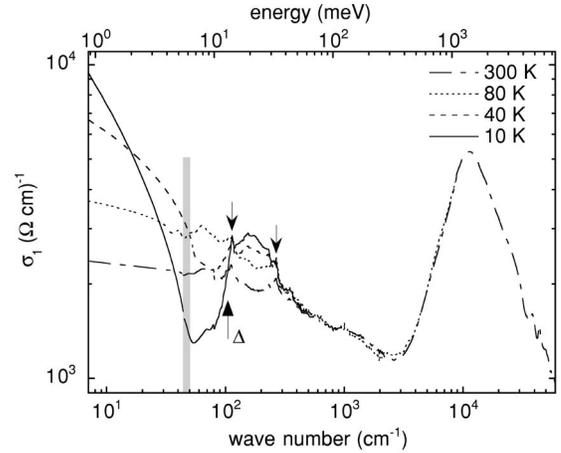

FIG. 4. Dissipative part of the optical conductivity $\sigma_1(\omega)$ at several temperatures. The vertical grey bar divides the data on the right side from the extrapolation of the data to low frequencies on the left. The downward-pointing arrows indicate the two strongest phonon peaks, which were observed at 114 and 267 cm^{-1}. Note the development of a gap-like feature with an onset at $\Delta \approx 100$ cm^{-1} (upward-pointing arrow) at temperatures $T < T^* \approx 70$ K.

Plotted in Fig. 4 is the dissipative part of the optical conductivity $\sigma_1(\omega)$ at four temperatures, as obtained from Kramers-Kronig analyis of the reflectance data. For clarity, only two of these temperatures were shown in the previous figure. Above T^*, in the incoherent regime, the frequency dependence of the conductivity can be described with the simple Drude formula, commonly used for metals: $\sigma_1(\omega) = \sigma_0/1 + \omega^2\tau^2$, where σ_0 is the dc conductivity and τ is the carrier relaxation time. At lower frequencies ($\omega \ll \tau^{-1}$) the conductivity is essentially constant, while at high frequencies ($\omega \gg \tau^{-1}$) it falls off as $\sigma \sim \omega^{-2}$. At higher frequencies, the conductivity increases to a maximum around 1.3 eV (10^4 cm^{-1}), which we believe is due to an interband transition. Below the characteristic temperature T^*, in the coherent (or Kondo lattice) regime, the conductivity gradually develops a narrow peak at zero frequency and a resonance, i.e., a sharp rise in $\sigma_1(\omega)$, with an onset around $\Delta = 13$ meV(100 cm^{-1}), indicated in the figure. The zero-frequency peak represents renormalized Drude response of heavy quasiparticles and is commonly found in heavy fermion materials.[26] The narrowness of the peak is due to the fact that the quasiparticle scattering rate, i.e., $1/\tau$ in the Drude formula, is strongly suppressed in this regime. One can estimate the quasiparticle effective mass based on the redistribution of spectral weight in the conductivity curves $\sigma_1(\omega)$ that takes place at low temperatures.[26] For the room-temperature data, the spectral weight is given by

$$\int_0^{\omega_c} \sigma_1(300\,K)d\omega = \frac{\omega_p^2}{8} = \frac{\pi n e^2}{2m_b}, \quad (3)$$

where the upper limit $\omega_c = 2730$ cm^{-1} is just below the onset of interband transitions, ω_p is the plasma frequency, n is

the carrier concentration, and m_b is the carrier-band mass. For the data at $T = 10$ K

$$\int_0^{\omega_h} \sigma_1(10\,K)d\omega = \frac{(\omega_p^*)^2}{8} = \frac{\pi n e^2}{2m^*}, \quad (4)$$

where $\omega_h = 54$ cm^{-1} is defined as the minimum in $\sigma_1(\omega)$ associated with the resonance at low temperatures, ω_p^* is the quasiparticle plasma frequency, and m^* the quasiparticle effective mass. Taking the ratio of the spectral weights at room temperature and 10 K, we estimate $m^*/m_b \approx 17$. The quasiparticle effective mass estimated from previous low-temperature specific heat measurements[18] is $m^*/m_e \approx 27$, where m_e is the free electron mass. This implies that the carrier-band mass at room temperature is slightly enhanced with $m_b \approx 1.7 m_e$. Using this value for m_b in Eq. (3), we obtain $n \approx 2.8 \times 10^{21}$ cm^{-3}, which is in good agreement with the carrier concentration of 3×10^{21} cm^{-3} estimated from Hall effect measurements. Other notable features in the data are narrow peaks at 114 and 267 cm^{-1} (marked by arrows), which we ascribe to phonon modes. Similar measurements on samples of RFe$_4$P$_{12}$ (R = La, Ce, Th, U) clearly show common phonon peaks, some of which may be associated with the "rattling" of the filled atom.[27] More detailed measurements (not shown) indicate that the resonance (Δ) does not shift appreciably in energy as a function of temperature between 10 and 70 K. We propose that the origin of this feature is a pseudogap in the density of states of the quasiparticles that opens in the vicinity of the Fermi level at low temperatures ($T < T^*$). These quasiparticles are admixtures of conduction electrons and Yb f electrons, renormalized by electron-electron interactions. Hybridization between the f level and conduction electron states becomes strong below T^*, producing heavy quasiparticles and a pseudogap of energy $\Delta \approx 13$ meV, which is probed by optical measurements. Metallic, holelike conduction in YbFe$_4$Sb$_{12}$ at low tempera-

tures can be explained if the Fermi energy E_F lies within the lower of the two split hybridized bands. A forthcoming article focusing on these and other optical reflectivity results will discuss this model in more detail.[28]

Similar features are seen in HF compounds such as UPt_3 (see Ref. 29) in which the formation of a (pseudo)gap in the quasiparticle density of states at low temperatures is ascribed to magnetic correlations, and also in the HF superconductor URu_2Si_2 in which the formation of a partial gap at the Fermi surface is brought about by the occurrence of a spin-density wave.[30,31] Clearly, much more remains to be studied regarding the nature of the gap in the electronic density of states that occurs in HF systems, and its relationship to the hybridization band gap that is proposed in materials such as UFe_4P_{12} and $Ce_3Bi_4Pt_3$.

IV. SUMMARY

Thermoelectric transport measurements indicate that $YbFe_4Sb_{12}$ is a hole-doped metal with low-carrier density. Coherence effects due to strong electronic correlations are evident in the electrical resistivity, magnetoresistance and the Seebeck coefficient below the coherence temperature $T^* \approx 70$ K. Relatively large values of the electrical resistivity lead to a low value for the thermoelectric figure of merit:

$ZT < 0.02$ below $T = 300$ K. Infrared and optical reflectivity studies show the onset of coherence as reveal a gaplike feature in the ac conductivity below a characteristic temperature T^*, which is ascribed to electronic hybridization effects. Future studies on Yb-filled skutterudites will aim to tailor the electronic conduction (via chemical doping) and/or reduce the thermal conduction (via partial filling of the Yb site) in exploring the metallurgical phase space for new thermoelectric materials. Optical studies hold great promise in elucidating the band structure of these materials and in answering long-standing questions regarding the nature of the f-electron many-body resonance near E_F and of band gaps due to electronic hybridization effects.

[1] W. Jeitschko and D. Braun, Acta Crystallogr., Sect. B: Struct. Crystallogr. Cryst. Chem. **33**, 3401 (1977).

[2] M.E. Danebrock, C.B.H. Evers, and W. Jeitschko, J. Phys. Chem. Solids **57**, 381 (1996).

[3] G.P. Meisner, Physica **108**, 763 (1981).

[4] G.P. Meisner, M.S. Torikachvili, K.N. Yang, M.B. Maple, and R.P. Guertin, J. Appl. Phys. **57**, 3073 (1985).

[5] D.T. Morelli and G.P. Meisner, J. Appl. Phys. **77**, 3777 (1995).

[6] D.A. Gajewski, N.R. Dilley, E.D. Bauer, E.J. Freeman, R. Chau, M.B. Maple, D. Mandrus, B.C. Sales, and A.H. Lacerda, J. Phys.: Condens. Matter **10**, 6973 (1998).

[7] C. Sekine, T. Uchiumi, I. Shirotani, and T. Yagi, Phys. Rev. Lett. **79**, 3218 (1997).

[8] B.C. Sales, D. Mandrus, and R.K. Williams, Science **272**, 1325 (1996).

[9] J.P. Fleurial, T. Caillat, and A. Borshchevsky, in *Thirteenth International Conference on Thermoelectrics, Kansas City, 1994*, edited by D. Mathiprakasan (AIP, New York, 1999), p. 40.

[10] B.C. Sales, D. Mandrus, B.C. Chakoumakos, V. Keppens, and J.R. Thompson, Phys. Rev. B **56**, 15 081 (1997).

[11] D.T. Morelli, G.P. Meisner, C. Baoxing, H. Siqing, and C. Uher, Phys. Rev. B **56**, 7376 (1997).

[12] C. Baoxing, X. Jun-Hao, C. Uher, D.T. Morelli, G.P. Meisner, J.P. Fleurial, T. Caillat, and A. Borshchevsky, Phys. Rev. B **55**, 1476 (1997).

[13] G.S. Nolas, J.L. Cohn, and G.A. Slack, Phys. Rev. B **58**, 164 (1998).

[14] G.A. Slack and V.G. Tsoukala, J. Appl. Phys. **76**, 1665 (1994).

[15] G.S. Nolas, G.A. Slack, D.T. Morelli, T.M. Tritt, and A.C. Ehrlich, J. Appl. Phys. **79**, 4002 (1996).

[16] V. Keppens, D. Mandrus, B.C. Sales, B.C. Chakoumakos, P. Dai, R. Coldea, M.B. Maple, D.A. Gajewski, E.J. Freeman, and S. Bennington, Nature (London) **395**, 876 (1998).

[17] G.D. Mahan and J.O. Sofo, Proc. Natl. Acad. Sci. USA **93**, 7436 (1996).

[18] N.R. Dilley, E.J. Freeman, E.D. Bauer, and M.B. Maple, Phys. Rev. B **58**, 6287 (1998).

[19] M.B. Maple, N.R. Dilley, D.A. Gajewski, E.D. Bauer, E.J. Freeman, R. Chau, D. Mandrus, and B.C. Sales, Phys. Rev. B **261**, 8 (1999).

[20] I. Isenberg, B.R. Russell, and R.F. Greene, Rev. Sci. Instrum. **19**, 685 (1948).

[21] R.B. Von Dreele, J.D. Jorgensen, and C.G. Windsor, J. Appl. Crystallogr. **15**, 581 (1982).

[22] M.S. Torikachvili, M.B. Maple, and G.P. Meisner, in *Proceedings of the 17th International Conference on Low Temperature Physics, LT-17*, edited by U. Eckern, A. Schmid, W. Weber, and H. Wuhl (North-Holland, Karlsruhe, Germany, 1984), p. 857.

[23] F. Blatt, P. Schroeder, C. Foiles, and D. Greig, *Thermoelectric Power of Metals* (Plenum, New York, 1976).

[24] S. Tripp, S. Spagna, and R.E. Sager (private communication).

[25] A. Leithe-Jasper, D. Kaczorowski, P. Rogl, J. Bogner, M. Reissner, W. Steiner, G. Wiesinger, and C. Godart, Solid State Commun. **109**, 395 (1999).

[26] L. Degiorgi, Rev. Mod. Phys. **71**, 687 (1999).

[27] S. Dordevic, N.R. Dilley, E.D. Bauer, D.N. Basov, M.B. Maple, and L. Degiorgi, Phys. Rev. B **60**, 11 321 (1999).

[28] S. Dordevic, D.N. Basov, N.R. Dilley, E.D. Bauer, and M.B. Maple, Phys. Rev. Lett. (to be published).

[29] S. Donovan, A. Schwartz, and G. Gruner, Phys. Rev. Lett. **79**, 1401 (1997).

[30] M.B. Maple, J.W. Chen, Y. Dalichaouch, T. Kohara, C. Rossel, M.S. Torikachvili, M.W. McElfresh, and J.D. Thompson, Phys. Rev. Lett. **56**, 185 (1986).

[31] L. Degiorgi, S. Thieme, H.R. Ott, M. Dressel, G. Gruener, Y. Dalichaouch, M.B. Maple, Z. Fisk, C. Geibel, and F. Steglich, Z. Phys. B **102**, 367 (1997).